International Journal of Thermophysics, Vol. 13, No. 3, 1992

Analysis of Multiwavelength Pyrometry Using Nonlinear Chi-Square Fits and Monte Carlo Methods

G. R. Gathers[1]

Received September 5, 1991

An analysis of multiwavelength pyrometry is made using Monte Carlo methods to evaluate the measurement error as a function of temperature for three, four, five, and six channels. Both a graybody and an emissivity with linear wavelength dependence are considered. χ^2 is calculated using the observed intensity in each channel and is minimized with respect to the temperature and the emissivity coefficients, using the Levenberg–Marquardt method. The influence of spectral span of the channels and the weight function used in the χ^2 fit are exmained. For the case of linear wavelength dependence, the solutions are found to be nonunique, even with six channels. The results show little improvement of precision with increasing number of channels beyond four channels when the nonlinear variable T is free. Both the spectral span and the weight function are shown to be important variables.

KEY WORDS: high temperature; Monte Carlo; pyrometry; radiation thermometry.

1. INTRODUCTION

Various authors have explored the use of multiwavelength pyrometry in an effort to improve the results by overdetermining the system [1–14]. The results to date have not indicated much improvement [2]. In this work Monte Carlo analysis is used to evaluate the scheme used by Radousky and Mitchell [9, 14] for a six-channel pyrometer. In the past, spectral fitting was done by calculating brightness temperatures for each channel and a mean temperature using a constant emissivity, then calculating the scatter of temperatures about the mean [15]. Emissivity and temperature were evaluated by minimizing the scatter. In the earliest work [15], the

[1] Lawrence Livermore National Laboratory, Livermore, California 94550, USA.

840/13/3-11

minimization was done by hand because it involved nonlinear least-squares methods.

More recently [15], a scheme has been devised using χ^2 to minimize the scatter observed in the intensities about those predicted for a given constant emissivity and temperature. The temperature and emissivity are varied to give a minimum χ^2 value, using the method of Levenberg and Marquardt [16], a modified version of the method of steepest descent. For this work, a wavelength dependent emissivity was chosen for greater generality.

2. METHOD

In the Levenberg–Marquardt (LM) method, the argument used in the χ^2 test (intensity here) is varied by a series of trials of the parameter vector composed of the adjustable parameters (emissivity coefficients and temperature here). The next guess for the parameter vector is determined by calculating the gradient of the χ^2 argument in the parameter space. This determines the direction to move in the parameter space. The magnitude of the change in the parameter vector is controlled by the change in χ^2 (if χ^2 increases, the magnitude of the change in the vector is reduced; otherwise it is increased.) As χ^2 approaches a minimum, the solution gradually becomes the result of solving the Hessian matrix.

Consider a multichannel pyrometer in which the response of each channel is assumed described by

$$R_i(T) = C \int_0^\infty D_i(\lambda)\, B_i(\lambda)\, \varepsilon(\lambda, T)\, W(\lambda, T)\, d\lambda \tag{1}$$

where $D_i(\lambda)$ and $B_i(\lambda)$ are the detector and optical response for channel i, respectively, $W(\lambda, T)$ is the Planck spectrum, and $\varepsilon(\lambda, T)$ is the emissivity. The constant C contains factors common to all channels, such as solid angle attenuation. We assume a linear wavelength dependence for the emissivity:

$$\varepsilon(\lambda, T) = a_0(T) + a_1(T)\lambda \tag{2}$$

Since solutions for a_0 and a_1 will be for a particular temperature T, we do not need to explicitly specify the form of the temperature dependence of a_0 and a_1. We assume that C can be determined by calibration if necessary and drop it here.

Define

$$F_i(T) = \int_0^\infty D_i(\lambda)\, B_i(\lambda)\, W(\lambda, T)\, d\lambda \tag{3}$$

and

$$H_i(T) = \int_0^\infty D_i(\lambda)\, B_i(\lambda)\, W(\lambda, T)\lambda\, d\lambda \tag{4}$$

where

$$W(\lambda, T) = \frac{c_1}{\lambda^5} \frac{1}{(e^{c_2/\lambda T} - 1)} \tag{5}$$

and c_1 and c_2 are the standard radiation constants.

For later use, we calculate the derivatives of F_i and H_i with respect to temperature:

$$E_i(T) = dF_i(T)/dT, \qquad G_i(T) = dH_i(T)/dT \tag{6}$$

Now

$$\frac{dw(\lambda, T)}{dT} = \frac{c_1 c_2}{\lambda^6 T^2} \frac{e^{c_2/\lambda T}}{(e^{c_2/\lambda T} - 1)^2} \tag{7}$$

so that

$$E_i(T) = \frac{c_1 c_2}{T^2} \int_0^\infty D_i(\lambda)\, B_i(\lambda) \frac{e^{c_2/\lambda T}}{(e^{c_2/\lambda T} - 1)^2} \frac{d\lambda}{\lambda^6} \tag{8}$$

and

$$G_i(T) = \frac{c_1 c_2}{T^2} \int_0^\infty D_i(\lambda)\, B_i(\lambda) \frac{e^{c_2/\lambda T}}{(e^{c_2/\lambda T} - 1)^2} \frac{d\lambda}{\lambda^5} \tag{9}$$

$$R_i(T) = c[a_0 F_i(T) + a_1 H_i(T)] \tag{10}$$

$$\left(\frac{\partial R_i}{\partial T}\right)_{a_0, a_1} = c[a_0 E_i(T) + a_1 G_i(T)] \tag{11}$$

$$\left(\frac{\partial R_i}{\partial a_0}\right)_{a_1, T} = cF_i(T) \tag{12}$$

$$\left(\frac{\partial R_i}{\partial a_1}\right)_{a_0, T} = cH_i(T) \tag{13}$$

We assume that the channels have variable precision so that we can write

$$\chi^2(\vec{a}) = \sum_{i=1}^{n} \frac{1}{\sigma_i^2} [R_i^* - R_i(\vec{a})]^2 \tag{14}$$

where $\vec{a} = (a_0, a_1, T)$, σ is the standard deviation for the channel, and the asterisk denotes experimental values. If we have a very narrow channel bandwidth, we can write

$$\int_0^\infty D_i(\lambda)\, B_i(\lambda)\, W(\lambda, T)\, d\lambda \cong c_i W(\lambda_i, T) \tag{15}$$

$$\int_0^\infty D_i(\lambda)\, B_i(\lambda)\, W(\lambda, T)\lambda\, d\lambda \cong c_i \lambda_i W(\lambda_i, T) \tag{16}$$

where λ_i is the average wavelength of the channel. We thus have

$$F_i(T) \cong c_i W(\lambda_i, T) = \frac{c_i c_1}{\lambda_i^5} \frac{1}{(e^{c_2/\lambda_i T} - 1)} \tag{17}$$

$$H_i(T) \cong c_i \lambda_i W(\lambda_i, T) = \frac{c_i c_1}{\lambda_i^4} \frac{1}{(e^{c_2/\lambda_i T} - 1)} \tag{18}$$

Similarly,

$$E_i(T) \cong \frac{c_i}{\lambda_i^6} \frac{c_1 c_2}{T^2} \frac{e^{c_2/\lambda_i T}}{(e^{c_2/\lambda_i T} - 1)^2} \tag{19}$$

$$G_i(T) \cong \frac{c_i}{\lambda_i^5} \frac{c_1 c_2}{T^2} \frac{e^{c_2/\lambda_i T}}{(e^{c_2/\lambda_i T} - 1)^2} \tag{20}$$

If all channels have the same spectral shape and width, we can absorb the factors c_i into the normalizing constant. We consider a normalized calculation and use the calibration constant to normalize the experimental intensity for each channel. We then have

$$R_i(T) \cong (a_0 + a_1 \lambda_i) \frac{c_1}{\lambda_i^5} \frac{1}{(e^{c_2/\lambda_i T} - 1)} \tag{21}$$

$$\left(\frac{\partial R_i}{\partial T}\right)_{a_0, a_1} \cong (a_0 + a_1 \lambda_i) \frac{c_1 c_2}{\lambda_i^6 T^2} \frac{e^{c_2/\lambda_i T}}{(e^{c_2/\lambda_i T} - 1)^2} \tag{22}$$

$$\left(\frac{\partial R_i}{\partial a_0}\right)_{a_1, T} \cong \frac{c_1}{\lambda_i^5} \frac{1}{(e^{c_2/\lambda_i T} - 1)} \tag{23}$$

$$\left(\frac{\partial R_i}{\partial a_1}\right)_{a_0, T} \cong \frac{c_1}{\lambda_i^4} \frac{1}{(e^{c_2/\lambda_i T} - 1)} \tag{24}$$

For channels of variable width and shape, we have, in summary,

$$R_i(T) = a_0 F_i(T) + a_1 H_i(T) \tag{25}$$

$$\left(\frac{\partial R_i}{\partial T}\right)_{a_0, a_1} = a_0 E_i(T) + a_1 G_i(T) \tag{26}$$

$$\left(\frac{\partial R_i}{\partial a_0}\right)_{a_1, T} = F_i(T) \tag{27}$$

$$\left(\frac{\partial R_i}{\partial a_1}\right)_{a_0, T} = H_i(T) \tag{28}$$

The integrals $F_i(T)$, $H_i(T)$, $E_i(T)$, and $G_i(T)$ can be tabulated for linear interpolation to obtain the value for a given temperature.

A code was written to generate artificial data for a linear ramp of temperature versus time over the temperature range 1500 to 20,000 K. After calculating the artificial data, random errors may be injected. Uniformly distributed random relative errors of a specified percentage of the intensity or random errors proportional to a given percentage of the maximum signal in a channel can be introduced (i.e., for the relative errors, if 2% errors are specified, the predicted intensity at a given time point is multiplied by a random number uniformly distributed in the range 0.98–1.02). A fresh random number is used for each channel at a given time, and for successive times. Some authors have examined the statistical improvement from increasing the number of channels using only 10 runs [2]. Since one is looking for a second-order effect (variation in the variance), results based on only 10 samples are not likely to be statistically significant. Gardner and Jones [3] gave a derivation of the variance in the fitted temperature for multiwavelength pyrometry using the Wien approximation, which shows that the precision should improve approximately proportional to the square root of the number of channels. Unfortunately, the derivation is flawed by reference to a result that is only valid when the curvature matrix for χ^2 is diagonal, and it is not diagonal for their basis. Problems using 500 runs were examined for the degree of scatter in the standard deviations. Since a ramp of temperature versus time is used, curve-fitting methods can be used to smooth the results for 100 runs. So long as relatively smooth temperature dependence is observed, the smoothed 100 run results give conclusions equivalent to those for 500 runs, without the greater computer time expense. This makes it possible to explore more variables.

Artificial data were generated for 100 successive runs, using a randomly chosen seed for each run. A data reduction code written using the same algorithms as those presently used by Radousky et al. was used to

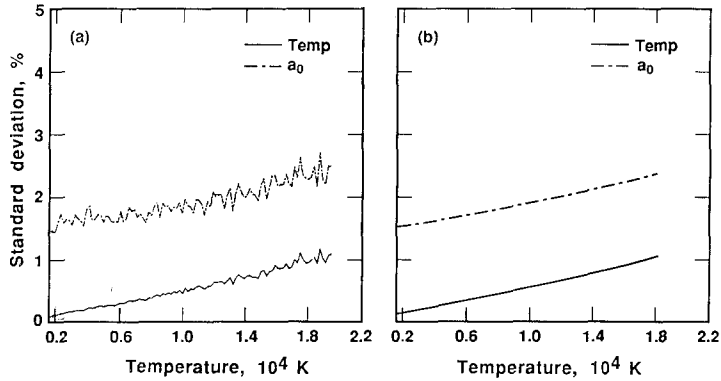

Fig. 1. Standard deviations of both the calculated emissivity and the calculated temperature versus the true temperature for a three-channel pyrometer with wavelengths at 254, 450, and 800 nm. Two percent uniformly distributed random relative errors and a graybody with emissivity 0.5 were used to generate the data. The LM method was used with both emissivity and temperature free. χ^2 was calculated using standard deviations equal to the signal level in a channel for each point. (a) Raw results; (b) smoothed results.

process the artificial data. The resulting temperature-versus-time curves from the 100 data sets are used to perform statistical analysis. At each time point, the 100 temperatures and emissivity coefficients are used to calculate the mean and standard deviation for each of these parameters. Since the original temperature corresponding to a given time point is known, the standard deviation for each parameter (a_0, a_1, T) can be correlated to a given temperature.

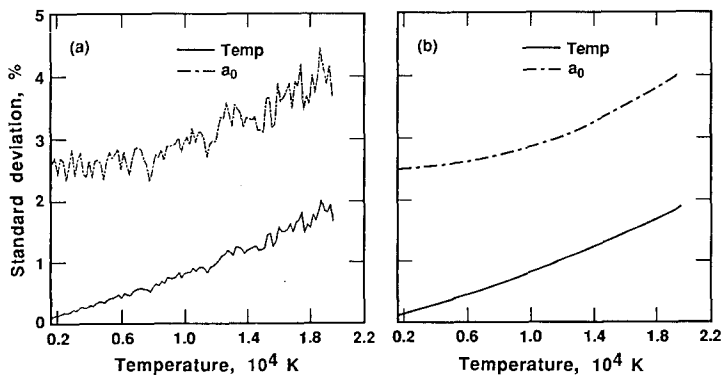

Fig. 2. Standard deviations of both the calculated emissivity and the calculated temperature versus the true temperature for a three-channel pyrometer with wavelengths at 310, 450, and 600 nm. All other parameters are the same as in Fig. 1. One hundred runs were used in both Figs. 1 and 2. (a) Raw results; (b) smoothed results.

3. RESULTS

The pyrometer described by Radousky and Mitchell [14] uses six wavelengths at 254, 310, 370, 450, 600, and 800 nm. The channel bandwidths are approximately 2 nm. Calibration of the instrument is made *in situ* with a standard lamp. The analytic fitting method used here is the one currently in use by Radousky and Mitchell [14] with one generalization: a linear wavelength dependence for the emissivity. A typical emissivity dependence for the assumed target was taken as 0.4 for the intercept a_0 and $-4\times10^{-4}\,\mathrm{nm}^{-1}$ for the wavelength coefficient a_1. No temperature dependence for the coefficients was used. Two percent uniformly distributed random relative errors were used in the analysis. First, analysis was per-

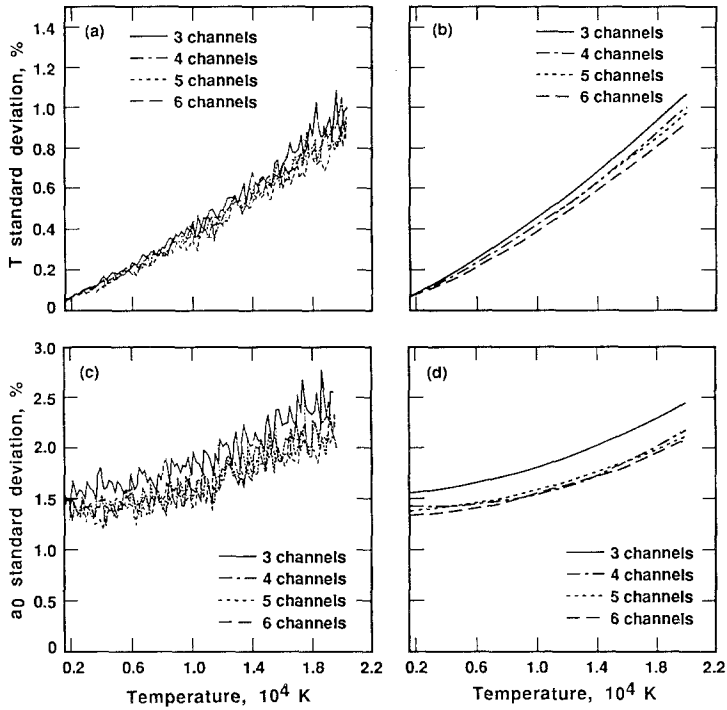

Fig. 3. Standard deviations of both the calculated emissivity and the calculated temperature versus the true temperature for three, four, five, and six channels. A graybody with emissivity 0.5 and 2% uniformly distributed random relative errors were used to generate the data. The LM method with both emissivity and temperature free was used, with the standard deviations for the χ^2 calculation equal to the signal level in a channel for each point. One hundred runs were used. (a) Raw T results; (b) smoothed T results; (c) raw ε results; (d) smoothed ε results.

formed both for narrow-band channels and for Gaussian channels with a full width at half-maximum (FWHM) of 50 nm. All six channels were used in the comparison. Comparison of the results for the two cases showed no significant differences. One can therefore either use relatively wide channels, to increase the sensitivity of the instrument, or use narrow-band channels, to decrease the possibility of recording possible line radiation which could be present.

The influence of the extent of the spectral span of the channels was examined, using three channels at 254, 450, and 800 nm and at 310, 450, and 600 nm. A graybody ($a_1 = 0$) with an emissivity of 0.5 was used for the analysis. Two percent uniformly distributed random relative errors were used, and the LM method was used with both emissivity and the temperature free to vary simultaneously. The standard deviation of each channel was taken proportional to the signal in the channel for each time point, consistent with the introduction of relative errors in the problem generation. Figure 1 shows the results for 254, 450, and 800 nm. Figure 2 shows the results for 310, 450, and 600 nm. It can be seen that decreasing the spectral span of the channels by about half produces an increase of about 70% in the standard deviations. Spectral span is thus seen to have a major influence. For studies of the statistical improvement due to increasing number of channels, therefore, the same spectral span was used in each case. For three channels the wavelengths were 254, 450, and 800 nm. For four channels the wavelengths were 254, 450, 600, and 800 nm, and for five channels the wavelengths used were 254, 370, 450, 600, and 800 nm.

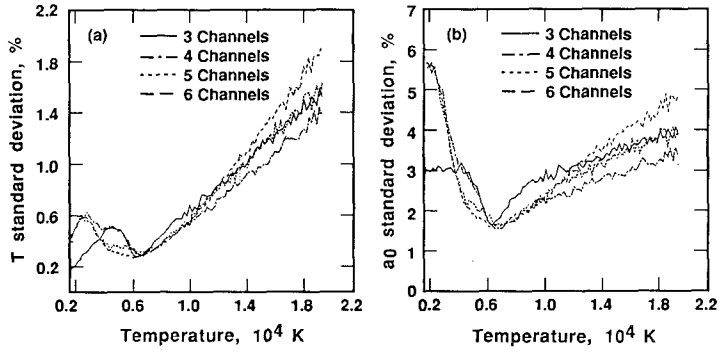

Fig. 4. Standard deviations of both the calculated emissivity and the calculated temperature versus the true temperature for three, four, five, and six channels. All parameters are the same as in Fig. 3, except that the standard deviations in the χ^2 calculation were all set to unity, and 500 runs were used. (a) Temperature; (b) emissivity.

3.1. Graybody Studies

The importance of the correct weight function in the χ^2 fits is shown in Figs. 3 and 4. Figure 3 shows a graybody with emissivity 0.5 and standard deviation in each channel set equal to the experimental measurement value in the channel at each time point. Two percent uniformly distributed random relative errors were used in generating the data. The LM method with both emissivity and temperature free was used. Results are shown for three, four, five, and six channels. Temperature T, the nonlinear variable, is free, and essentially normal statistical behavior is observed (increasing the number of channels improves the precision of the measure-

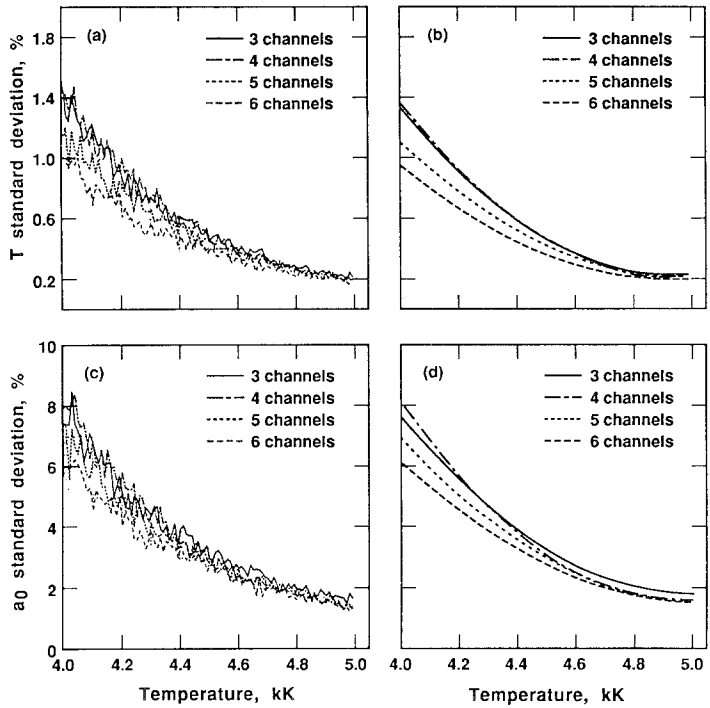

Fig. 5. Standard deviations of both the calculated emissivity and the calculated temperature versus the true temperature for three, four, five, and six channels. Random absolute errors in the band plus or minus 2% of the maximum signal seen in each channel were used. The temperature range considered was restricted to 4000–5000 K to prevent the range of relative error from dominating the dependence on number of channels in the figure. χ^2 was calculated using standard deviation equal to the maximum signal seen in each channel. A graybody with emissivity 0.5 was used. (a) Raw T results; (b) smoothed T results; (c) raw ε results; (d) smoothed ε results.

ment), but the improvement is less than would be expected with only linear dependence in the parameters. Figure 4 shows the same data, reduced with the standard deviations for each channel set to unity. The statistical behavior is abnormal. At about 6500 K, a favored result is observed, corresponding to the case where the channels are about equally distributed on either side of the spectral maximum. There is little dependence on the number of channels used. At other temperatures, increasing the number of channels beyond four actually degrades the precision. Five hundred runs were used in generating the results in Fig. 4.

Figure 5 shows results using uniformly distributed random absolute errors in the band plus or minus 2% of the maximum signal seen in a channel. This is characteristic of errors due to trace width for data recorded on an oscilloscope or to discriminator level spacing using a digital waveform recorder. At lower deflections or discriminator levels (lower temperatures), as expected, the relative error increases. The temperature range

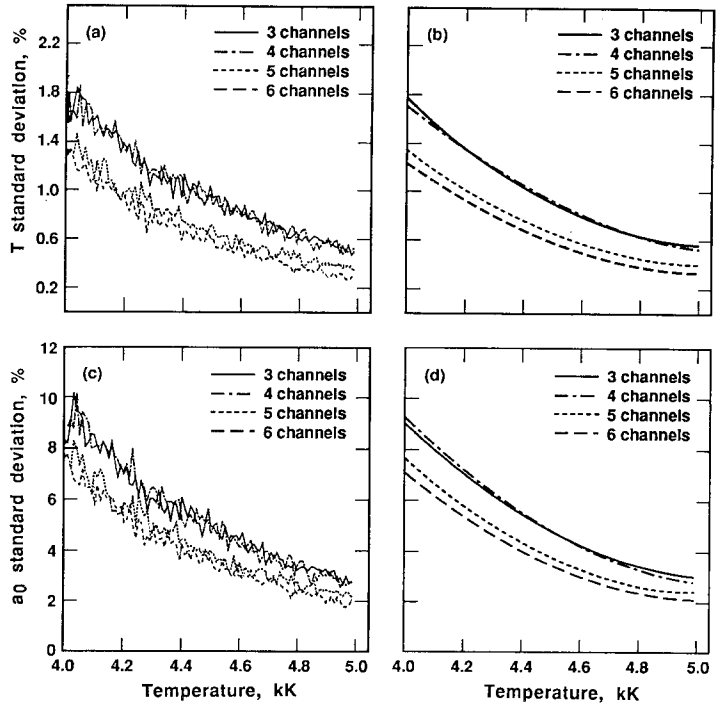

Fig. 6. Standard deviations of the calculated emissivity and temperature versus true temperature. All parameters are the same as in Fig. 5 except that the standard deviations were all set to unity. (a) Raw T results; (b) smoothed T results; (c) raw ε results; (d) smoothed ε results.

considered was restricted to the range 4000 to 5000 K to keep the range of the relative error from dominating the dependence on the number of channels in the figure. The χ^2 fits used standard deviations equal to the maximum signal seen in each channel. Essentially normal statistical behavior is observed, and with only two variables, the improvement varies approximately with the square root of the number of channels, even though the temperature is a nonlinear variable.

Figure 6 shows results using the same data as in Fig. 5, but with the standard deviations set to unity. For the graybody, using the wrong weight function increases the standard deviation of the solutions, but approximately normal statistical behavior is observed.

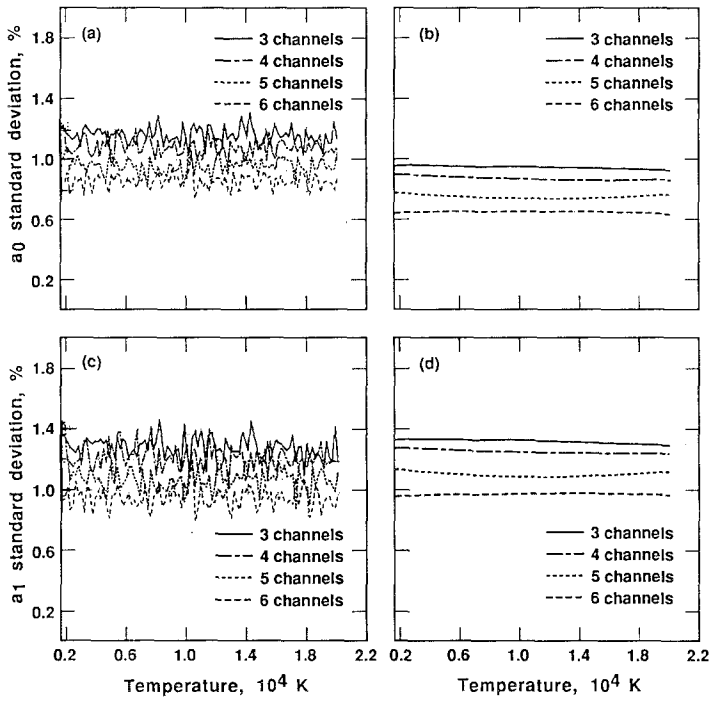

Fig. 7. Standard deviations of the calculated emissivity coefficients versus the true temperature for a linear wavelength dependence. $a_0 = 0.4$, $a_1 = -4 \times 10^{-4}\,\mathrm{nm}^{-1}$, and 2% uniformly distributed random relative errors were used to generate the data. The LM method was used with T locked to the exact value at each point. Both a_0 and a_1 were allowed to vary. The standard deviations were taken equal to the signal level in a channel for each point. (a) Raw a_0 results; (b) smoothed a_0 results; (c) raw a_1 results; (d) smoothed a_1 results.

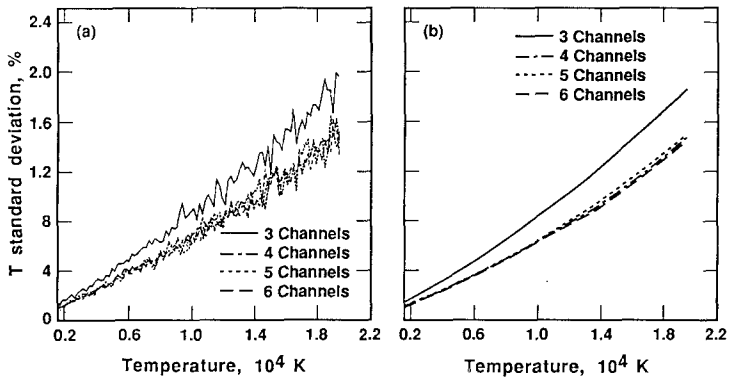

Fig. 8. Standard deviation of the calculated temperature versus true temperature for a linear wavelength dependence. All parameters are the same as in Fig. 7, except that the temperature is also free to vary. (a) Raw results; (b) smoothed results.

3.2. Nongraybody Studies

An emissivity model of $\varepsilon = a_0 + a_1\lambda$ was used, with $a_0 = 0.4$ and $a_1 = -4 \times 10^{-4}\ \mathrm{nm}^{-1}$. The LM method was used, but only the linear variables a_0 and a_1 were allowed to vary. The temperature was set to the exact value for each time point. Two percent uniformly distributed random relative errors were used in generating the data, and the standard deviations were set to the signal level at each time point for each channel. Figure 7 shows the results. With the correct weight function and only the linear variables free, the statistical behavior is normal and the improvement with increasing

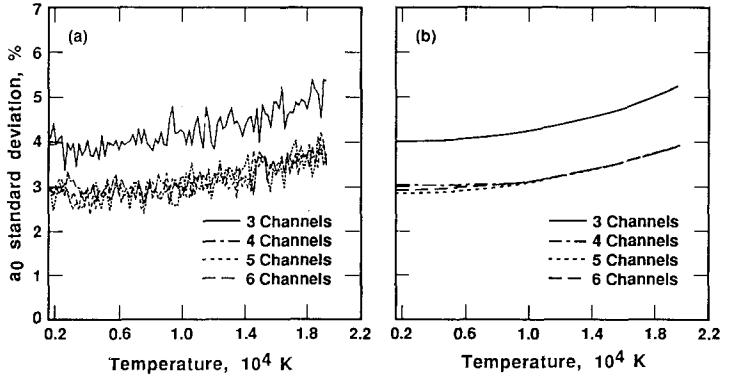

Fig. 9. Standard deviation of the calculated a_0 coefficient versus true temperature for a linear wavelength dependence. All parameters are the same as in Fig. 7, except that the temperature is also free to vary. (a) Raw results; (b) smoothed results.

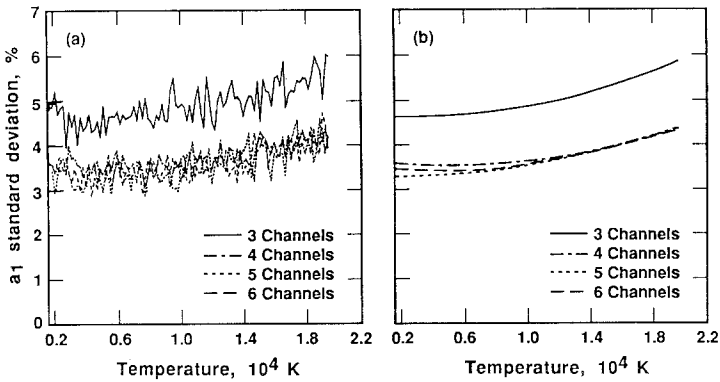

Fig. 10. Standard deviation of the calculated a_1 coefficient versus true temperature for a linear wavelength dependence. All parameters are the same as in Fig. 7, except that the temperature is also free to vary. (a) Raw results; (b) smoothed results.

number of channels is approximately proportional to the square root of the number of channels, as expected. Figures 8, 9, and 10 show the results for the same problem when the temperature is also allowed to vary. Statistical behavior is still essentially normal, but the standard deviations are four to five times larger for the emissivity coefficients, and for all three variables, there is little improvement beyond four channels.

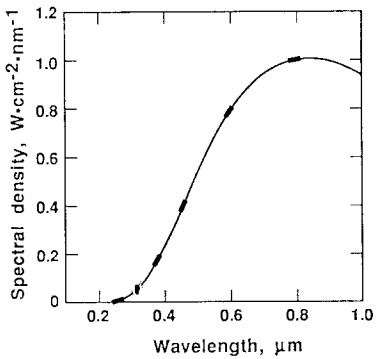

Fig. 11. Example of nonunique solutions for a six-channel pyrometer with the wavelengths 254, 310, 370, 450, 600, and 800 nm. One spectrum corresponds to $T = 4000$ K, $a_0 = 0.3$, and $a_1 = 6 \times 10^{-4}$ nm^{-1}. The other solution corresponds to $T = 4817.4$ K, $a_0 = -0.12523$, and $a_1 = 6.0491 \times 10^{-4}$ nm^{-1}. Over the wavelength range shown, the solutions are indistinguishable.

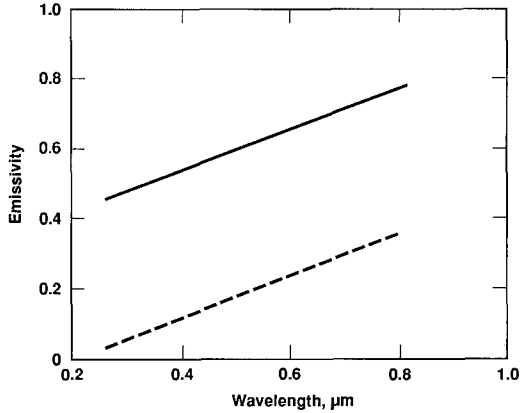

Fig. 12. Emissivity for the two solutions in Fig. 11. The solid curve is for the solution at 4000 K. The other curve corresponds to 4817.4 K.

4. NONUNIQUE SOLUTIONS

It should be noted that with a linear wavelength dependence for the emissivity, the solutions achieved are not unique. Figure 11 gives an illustrative example. With six channels all located on the blue side of the spectral maximum, there are at least two solutions that give an excellent fit with almost identical values for χ^2. There are no artificial errors involved. The spectrum was calculated for a temperature of 4000 K and emissivity coefficients $a_0 = 0.3$ and $a_1 = 6 \times 10^{-4}\,\mathrm{nm}^{-1}$. The second solution ($T = 4817.4$ K, $a_0 = -0.12523$, $a_1 = 6.0491 \times 10^{-4}\,\mathrm{nm}^{-1}$) was found using the LM method. Figure 12 shows the two emissivity curves. The emissivities for each case are physically reasonable for the wavelength range considered. For the first solution, the emissivity ranges from 0.45 to 0.78, while for the second, it ranges from 0.028 to 0.36. The only thing unusual about the second solution is that the emissivity is very low for the short wavelengths. In other situations, however, this might not occur.

5. CONCLUSIONS

The improvement in precision obtained by increasing the number of channels in a pyrometer and using spectral fit methods with χ^2 has been studied both for a graybody and for an emissivity with linear wavelength dependence. For a graybody, with random absolute errors in the band plus or minus 2% of the maximum signal seen in each channel, the standard deviations for both temperature and emissivity continue to show reduction

for six channels, but for 2% uniformly distributed random relative errors, little reduction in the emissivity standard deviation is seen beyond four channels.

For an emissivity with linear wavelength dependence, and 2% uniformly distributed random relative errors, little reduction in the standard deviation is seen for temperature or either emissivity coefficient beyond four channels.

It has also been shown that the spectral span of the channels should be as large as is practical, and the correct weight function should be used when fitting by the method of minimizing χ^2. The choice of bandwidth in the channels is decided by the need for sensitivity versus the need to avoid possible line radiation.

The Levenberg–Marquardt method was used, since it is almost the only general method available for finding the solutions required for the nonlinear least-squares fit. The method of locking temperature and solving the resulting linear equations for a_0 and a_1 and varying temperature separately was also evaluated but found to be rather unstable when used over a very large temperature range.

A serious problem of nonunique solutions for emissivity with linear wavelength dependence was demonstrated. Two separate physically reasonable solutions can be found with temperatures different by as much as 800 K.

ACKNOWLEDGMENT

This work was performed under the auspices of the U.S. Department of Energy by the Lawrence Livermore National Laboratory under Contract W-7405-ENG-48.

REFERENCES

1. G. A. Lyzenga and T. J. Ahrens, *Rev. Sci. Instrum.* **50**:1421 (1979).
2. J. L. Gardner, *High Temp. High Press.* **12**:699 (1980).
3. J. L. Gardner and T. P. Jones, *J. Phys. E Sci. Instrum.* **13**:306 (1980).
4. J. L. Gardner, T. P. Jones, and M. R. Davies, *High Temp. High Press.* **13**:459 (1981).
5. G. A. Lyzenga and T. J. Ahrens, *Rev. Sci. Instrum.* **76**:6282 (1982).
6. G. A. Lyzenga, T. J. Ahrens, W. J. Nellis, and A. C. Mitchell, *J. Chem. Phys.* **76**:6282 (1982).
7. J.-P. Hiernaut, R. Beukers, W. Heinz, R. Selfslag, M. Hoch, and R. W. Ohse, *High Temp. High Press.* **18**:617 (1986).
8. V. N. Snopko, *High Temp. (USSR)* **25**:724 (1987).
9. H. B. Radousky, in *Shock Waves in Condensed Matter, 1987*, S. C. Schmidt and N. C. Holmes, eds. (Elsevier, New York, 1988), pp. 89–94.

10. P. B. Coates, *High Temp. High Press.* **20**:433 (1988).
11. J.-P. Hiernaut, F. Sakuma, and C. Ronchi, *High Temp. High Press.* **21**:139 (1989).
12. J.-F. Babelot and M. Hoch, *High Temp. High Press.* **21**:79 (1989).
13. M. B. Boslough and T. J. Ahrens, *Rev. Sci. Instrum.* **60**:3711 (1989).
14. H. B. Radousky and A. C. Mitchell, *Rev. Sci. Instrum.* **60**:3707 (1989).
15. N. C. Holmes, Private communication.
16. W. H. Press, B. P. Flannery, S. A. Teukolsky, and W. T. Vetterling, *Numerical Recipes* (Fortran version) (Cambridge University Press, 1989), pp. 523–528.

Printed in Belgium